Electronic Supplementary Material (ESI) for Journal of Materials Chemistry A.

Supporting Information

Novel gas sensing platform based on a stretchable laser-induced graphene pattern with self-heating capabilities

Li Yang[a,b,‡], Ning Yi[c,‡], Jia Zhu[b], Zheng Cheng[d], Xinyang Yin[e], Xueyi Zhang[e], Hongli Zhu[d], Huanyu Cheng[b,c,f,*]

[a]Hebei Key Laboratory of Robot Perception and Human-robot Interaction, School of Mechanical Engineering, Hebei University of Technology, Tianjin 300401, China

[b]Department of Engineering Science and Mechanics, The Pennsylvania State University, University Park, PA, 16802, USA

[c]Department of Materials Science and Engineering, The Pennsylvania State University, University Park, PA, 16802, USA

[d]Department of Mechanical and Industrial Engineering, Northeastern University, Boston, MA, 02115, USA

[e]Department of Chemical Engineering, The Pennsylvania State University, University Park, PA, 16802, USA

[f]State Key Laboratory of Digital Manufacturing Equipment and Technology, Huazhong University of Science and Technology, Wuhan, Hubei, 430074, China

[‡]These authors contribute equally.

[*]To whom correspondence should be addressed. E-mail: huanyu.cheng@psu.edu

Experimental

Fabrication of the gas testing platform based on laser-induced graphene

A polyimide (PI) film (Kapton HN, 90 µm thickness) laminated on a water-soluble tape (3M, 5414 tapes) was first attached on glass slides by a double-sided tape. Upon direct CO_2 laser (Universal Laser, 10.6 µm) scribing with a power of 16 % and speed of 10 %, porous laser-induced graphene (LIG) patterns formed on the top surface of the PI by photothermal ablation. The same laser system with a lower power of 5 % and a lower scanning rate of 1 % enabled the cutting of LIG patterns. Immersing the resulting sample in water dissolved the water-soluble tape and released the LIG patterns from the glass substrate. Rinsing the LIG surface with ethanol and water subsequently with mild agitation removed the dust and contaminants. After attaching the LIG to a water-soluble tape with gentle pressure, a thin Ecoflex (Smooth-on, Ecoflex 00-30) layer with a thickness of 500 µm was cast on the back of PI surface and cured at 60 °C on a hot plate for one hour. Dissolving the water-soluble tape exposed the LIG pattern with two serpentine lines (width of 2 mm) and a single straight line with various lengths and widths. Coating the serpentine lines with silver ink (Novacentrix AJ-191) reduced their electrical resistances to provide electrical connection to the external data acquisition system. Drop casting nanomaterials such as MoS_2, rGO/MoS_2, or ZnO/CuO core/shell nanomaterials in the LIG single line sensing region completed the fabrication of a highly sensitive stretchable gas sensor.

Preparation of the ZnO/CuO core/shell nanomaterials

Intergrowth $Cu_2(nbdc)_2(dabco)$ on $Zn_2(nbdc)_2(dabco)$ was synthesized by the conventional seeded growth method. In a typical procedure, $Cu(NO_3)_2{\cdot}3H_2O$ was dissolved in

N,N-dimethylformamide (DMF). Next, acid linker 3-Nitrophthalic acid (3-nitrobenzenedicarboxylic acid, nbdc) was dissolved in DMF. Base (pyridine) was then added with micropipette into base linker dabco (1,4-diazabicyclo[2.2.2]octane) solution in DMF. 66 µL seed dispersion (0.1 % conventional $Zn_2(nbdc)_2(dabco)$ pillared metal-organic framework (MOF) suspension in DMF (wt %)) was added into the base solution. Once linkers and metal salt were completely dissolved, metal solutions and acid linkers were added into the seed solution. The final mixture with a molar ratio of metal salt: nbdc: dabco: base: DMF = 2.8: 2: 2: 40: 24000 was shaken on an orbital shaker at 200 rpm for 48 hours. The solid in the resulting suspension was separated using centrifugation (4000 RCF). The obtained bimetallic MOF was then used to prepare the mixed metal oxide nanomaterials. Intergrowth MOF $Cu_2(nbdc)_2(dabco)$-on-$Zn_2(nbdc)_2(dabco)$ of 100 mg was heated in N_2 (50 SCCM) at 400 °C (ramp rate of 1 °C/min) for 10 hours followed by dry air (50 SCCM) at 400 °C for another 10 hours. The obtained ZnO/CuO core/shell nanomaterials were cooled to room temperature in dry air.

Synthesis of rGO/MoS_2 composite

The rGO/MoS_2 composites were prepared by a solvothermal method. In brief, 24 mg MoO_3, 28 mg thioacetamide, and 0.2 g urea were dissolved in 16 ml ethanol with continuous magnetic stirring for 1 h, followed by adding 4 ml GO suspension of 3.5 mg/ml. Next, the well-mixed solution was transferred to an autoclave and loaded into a furnace (MTI). Heating the furnace to 200 °C and then the temperature was maintained for 16 h. Removing the autoclave from the oven rapidly cooled down the solution to room temperature and terminated the reaction. The as-prepared rGO/MoS_2 composite was collected and washed with deionized water and then ethanol, followed by storage in the mixture of deionized water and ethanol at the volume ratio of 1:1 before use.

The confined growth of the rGO/MoS_2 composites followed the same recipe as above. 12 mg MoO_3, 14 mg thioacetamide, and 0.1 g urea were dissolved in 8 ml ethanol with continuous magnetic stirring for 1 h, followed by adding 2 ml GO suspension of 3.5 mg/ml. After transferring the 10 ml reactant suspension into the autoclave reactor, 20 ml NaCl crystal fillers (Morton Salt, as-bought) were added into the reactor slowly with agitation. After the reactor was placed still for 5 min, the supernatant liquid was removed (the liquid existed only between the crystal fillers). After maintaining the temperature at 200 °C for 16 h, the as-prepared rGO/MoS_2 filled in the confined spaces formed by crystal fillers. The crystal fillers were dissolved by water to collect the products, and the obtained products were washed by deionized water for at least five times. Finally, the black dispersive rGO/MoS_2 product was dialyzed with deionized water for at least seven days using regenerated cellulose dialysis membranes until no smell.

Testing of gas sensors

The gas-sensing performance of various gas sensors was characterized in a static gas sensor testing system with a commercial computer-controlled SourceMeter (Keithley 2400, Keithley Instruments, USA). Different concentrations of NO_2 in the sealed chamber were prepared by diluting and well mixing the 100 ppm NO_2 calibration gas (GASCO) with the air in the chamber with a volume of 10 L. To demonstrate the conformal attachment of the gas sensors on human body, water was sprayed onto the wrist before the application. Surface tension between water and PDMS ensured the conformal contact. Informed consent was obtained from the participant before the experiment.

SEM imaging

The morphologies of the as-prepared rGO and rGO/MoS_2 were characterized by the SEM (Hitachi S4800) at an accelerating voltage of 10.0 kV.

Figures

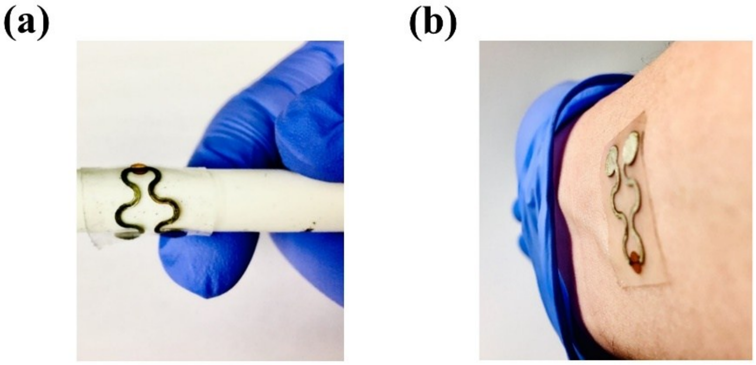

Figure S1. Optical images of the gas sensor **(a)** bent over a cylinder with a radius of 5.53 mm and **(b)** attached to the back surface of the hand.

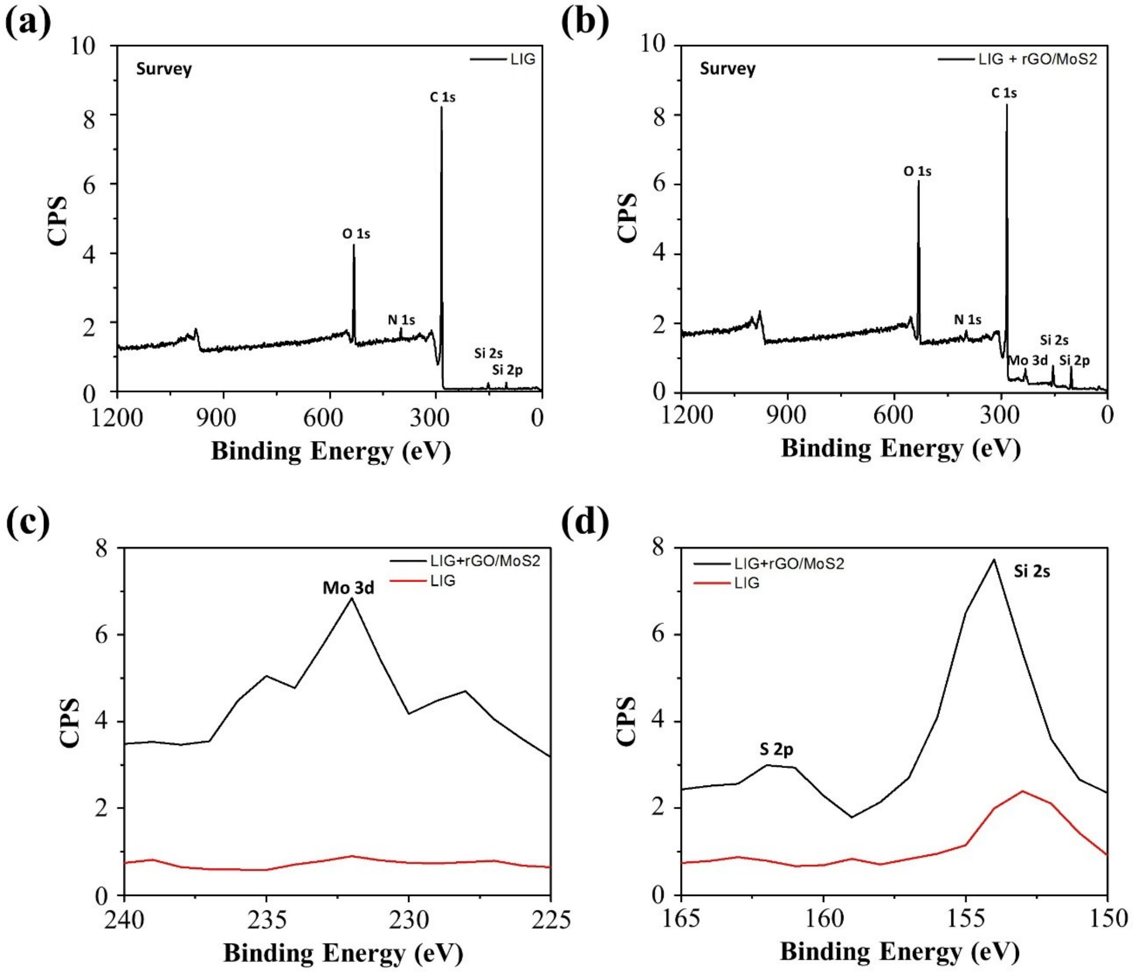

Figure S2. XPS survey scan for **(a)** bare LIG samples and **(b)** LIG with the addition of rGO/MoS_2 synthesized with the addition of NaCl crystals **(c)** the Mo 3d doublet centered at the binding energy of 232 eV and 228 eV **(d)** the S 2p peak centered at 162 eV.

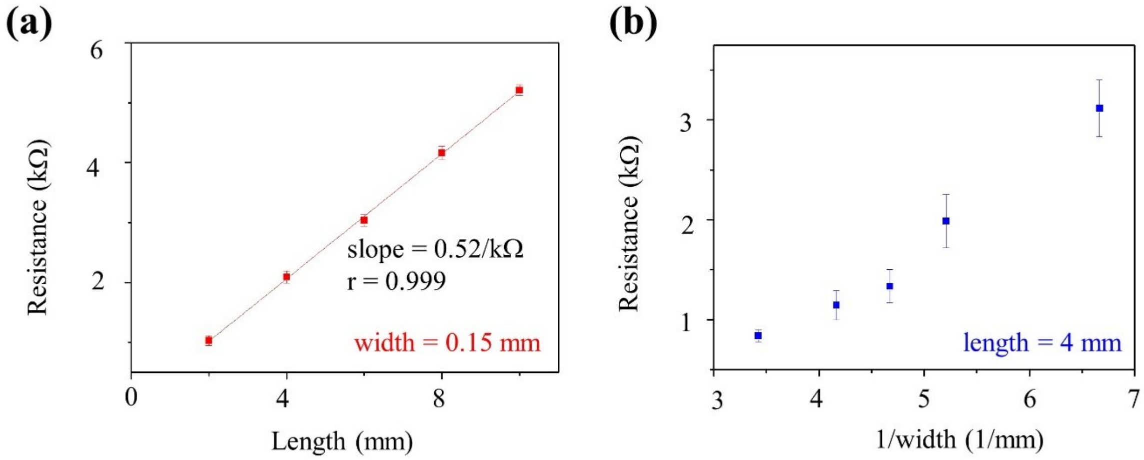

Figure S3. Dependence of the resistance of the LIG electrode on its **(a)** length and **(b)** width. The solid red line in **(a)** represents the linear fit to the experimental data. Calculating the slope gave a sheet resistance of 78 Ω/sq.

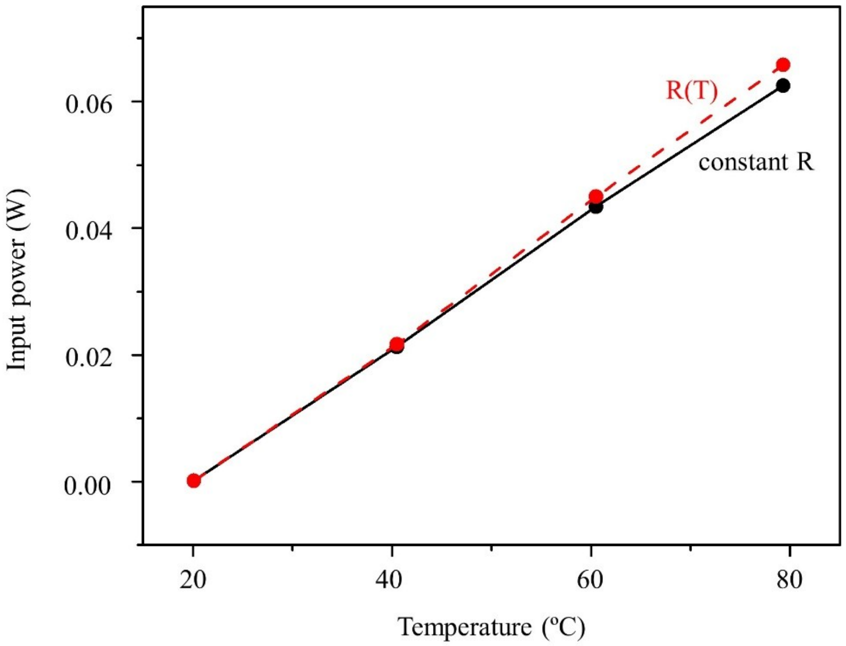

Figure S4. Dependence of the temperature in the LIG electrode from self-heating on the input power, in which the solid black line assumes a constant resistance over time and the dashed red line uses the real-time resistance that decreased with the increasing temperature.

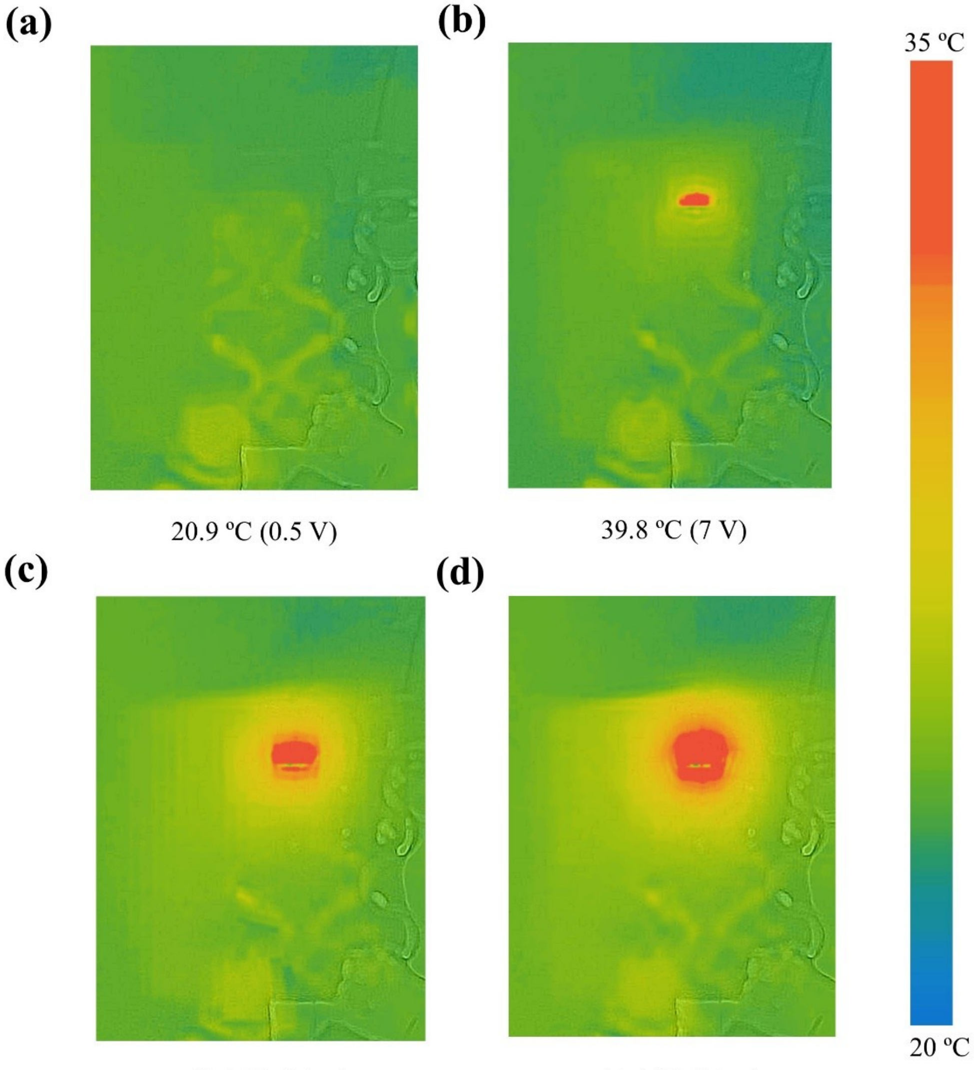

20.9 ºC (0.5 V)

39.8 ºC (7 V)

60.1 ºC (10 V)

80.1 ºC (12 V)

Figure S5. Spatial distributions of the temperature in the LIG electrode from different self-heating conditions.

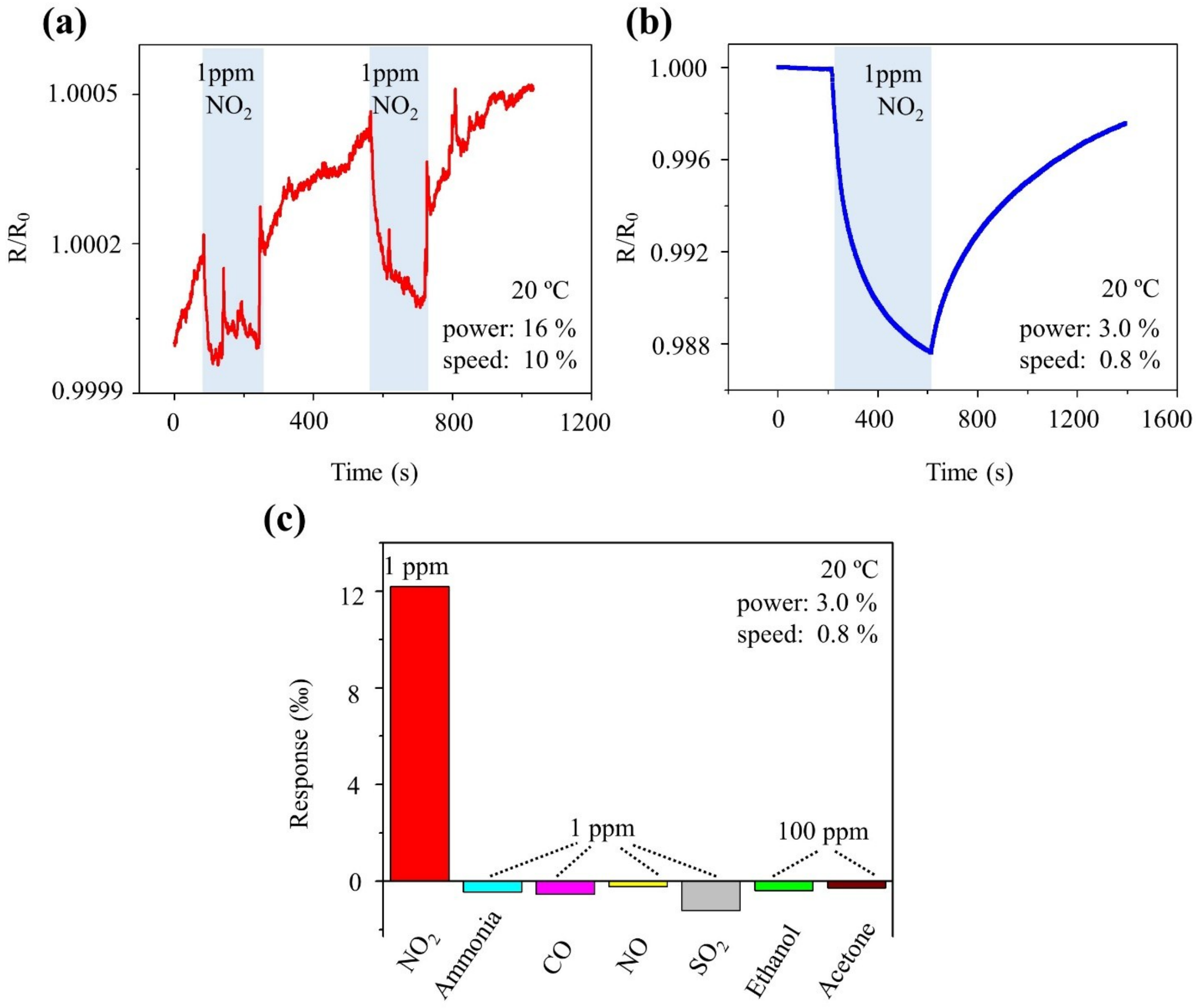

Figure S6. The gas-sensing performance of pristine LIG lines to NO$_2$ of 1 ppm at 20 ºC. Gas sensing response observed in the pristine LIG when **(a)** a power of 16 % and a speed of 10 % or **(b)** a power of 3% and a speed of 0.8 % were used in the laser scribing process. **(c)** The selectivity of the pristine LIG line in **(b)**.

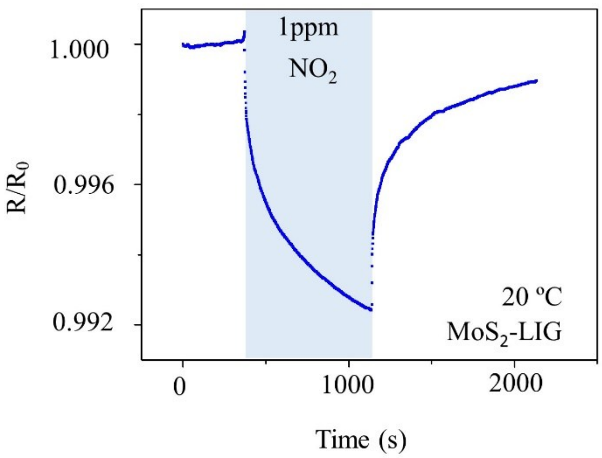

Figure S7. The response of the MoS$_2$-LIG gas sensor to NO$_2$ of 1 ppm at 20 ºC.

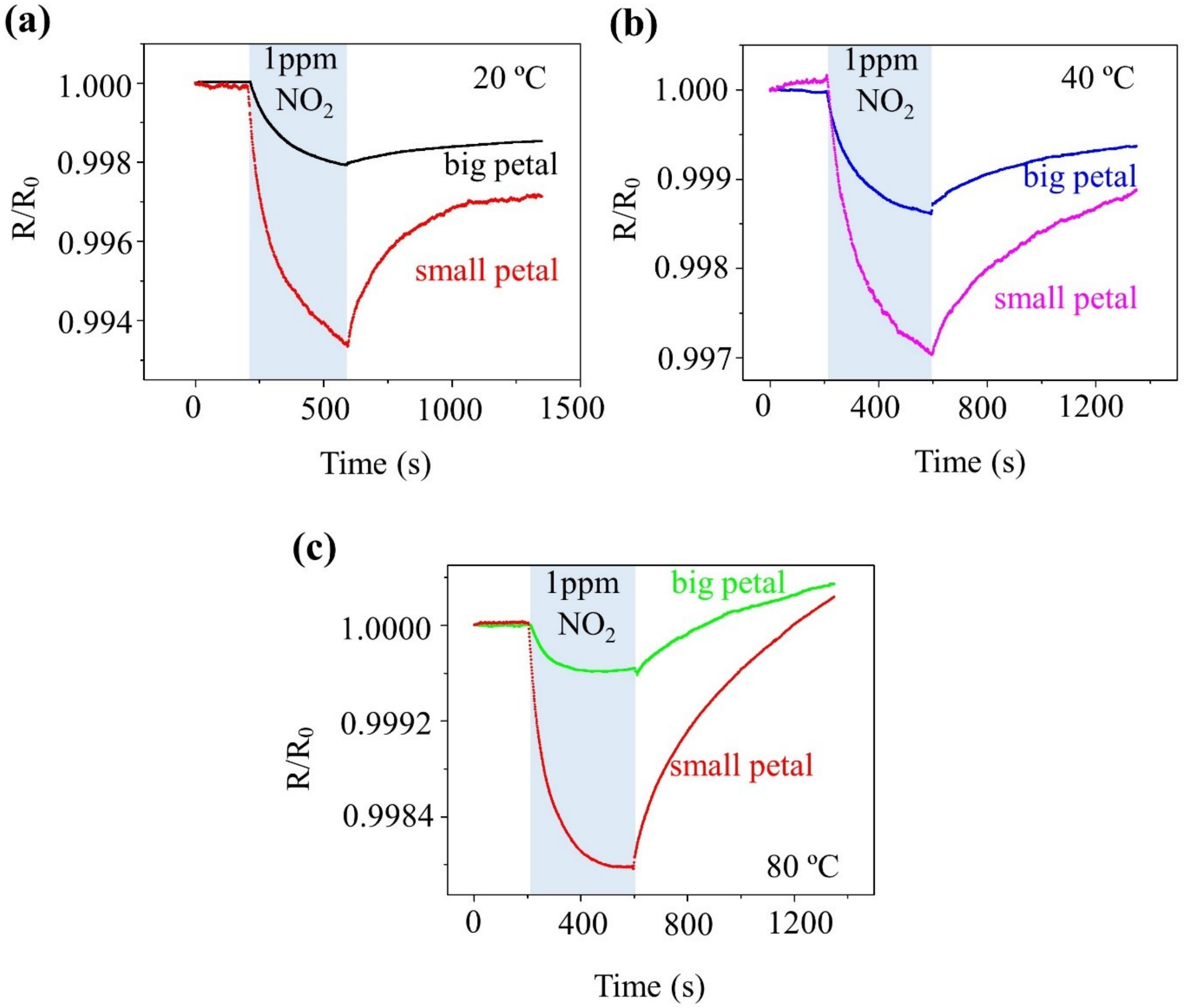

Figure S8. Comparison of the gas sensing performance between gas sensors with the big and small petal structures at **(a)** 20 ºC, **(b)** 40 ºC, and **(c)** 80 ºC from self-heating.

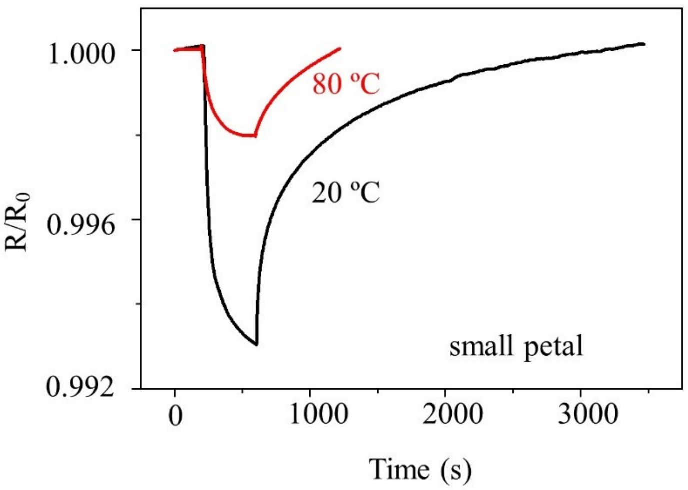

Figure S9. Comparison of the gas sensing performance of the LIG with the small petal structure evaluated at 20 ºC and 80 ºC with a complete recovery time.

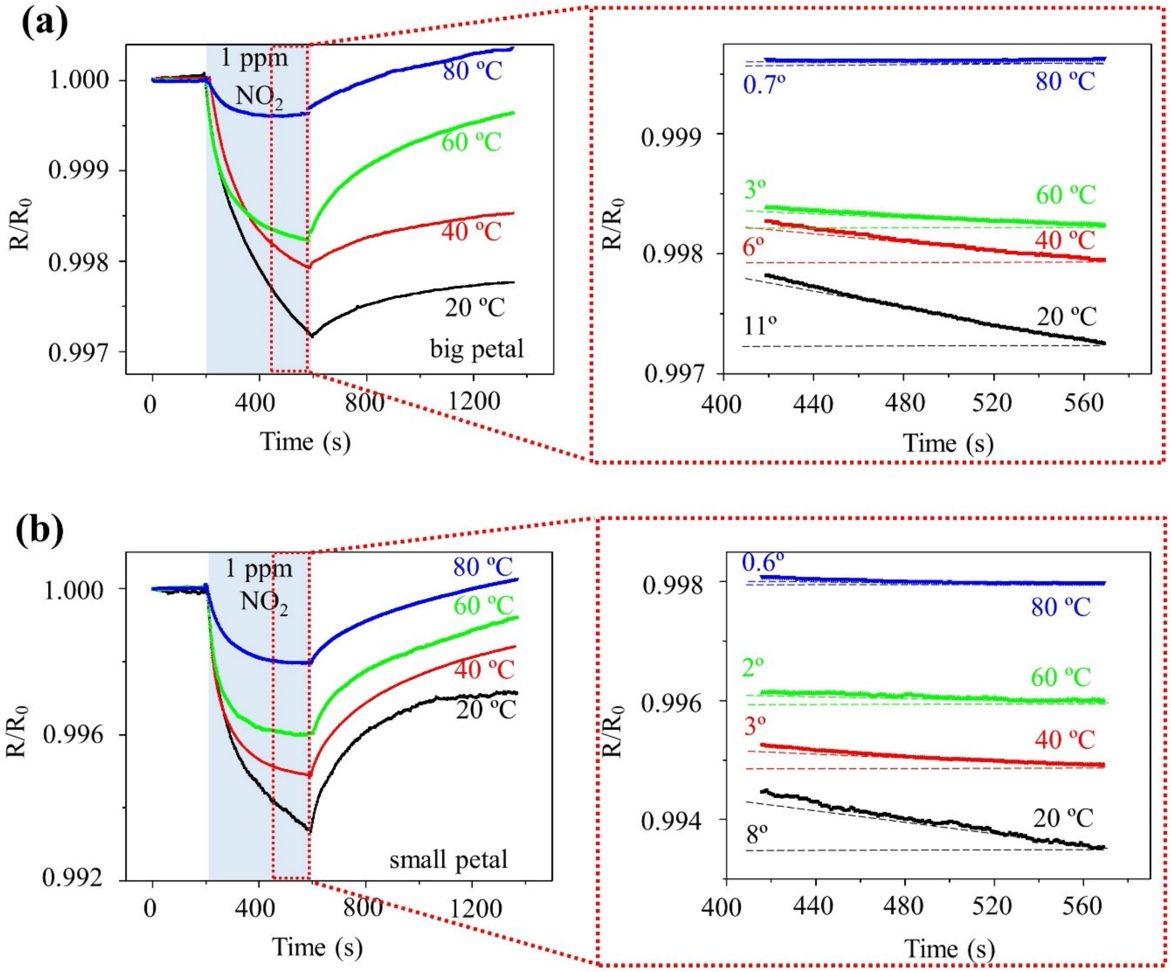

Figure S10. Comparison of the angle of the plateau calculated from response curves of gas sensors with the big and small petal structures at 20 ºC, 40 ºC, 60 ºC, and 80 ºC from self-heating.

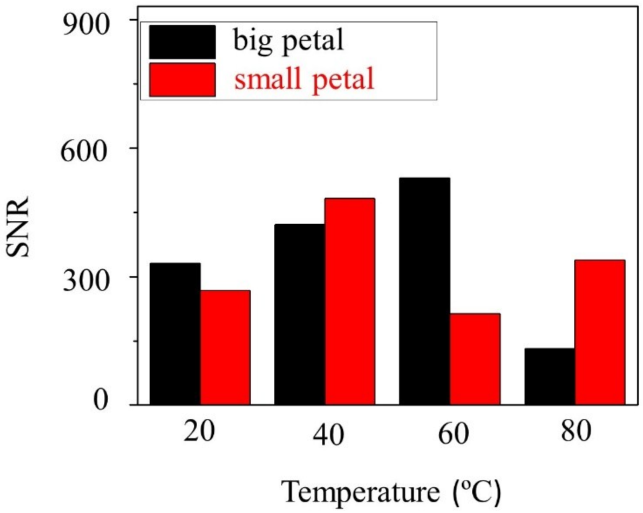

Figure S11. Comparison of the SNR between gas sensors with the big and small petal structures at different temperatures from self-heating.

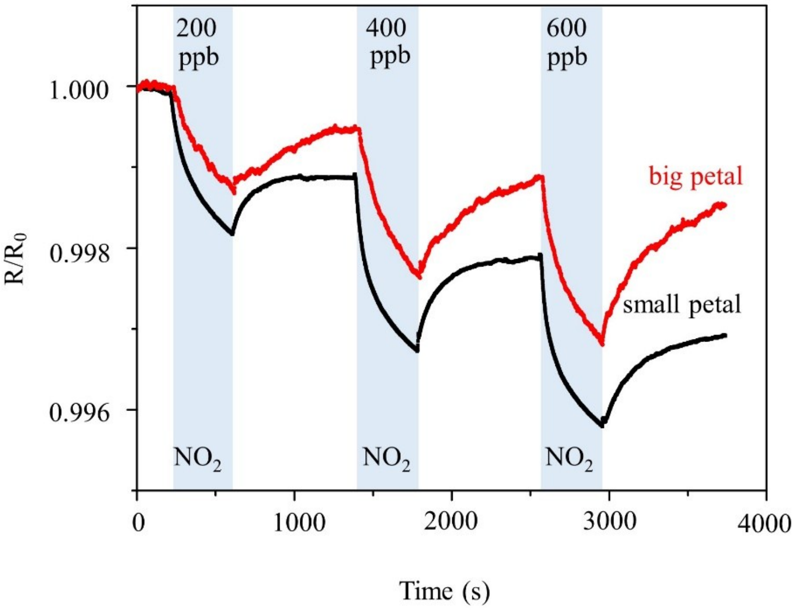

Figure S12. Dynamic response test of the gas sensors with the big and small petal structures in the presence of NO_2 from 200 ppb to 600 ppb.

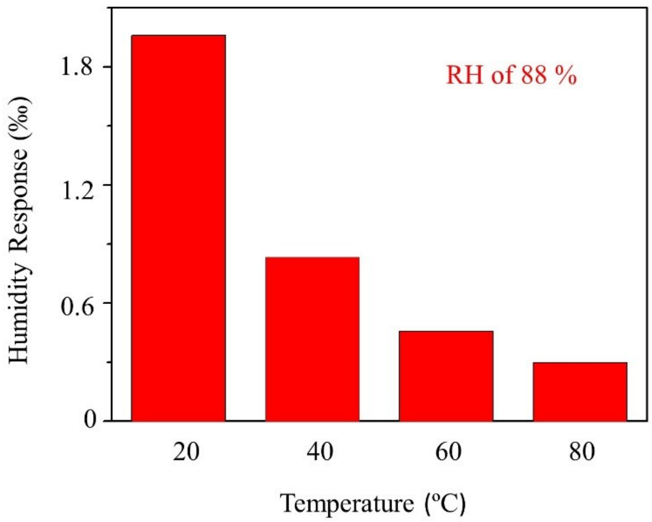

Figure S13. Effect of the high relative humidity (RH) of 88 % on the response of the rGO/MoS_2-LIG gas sensor at different temperatures.

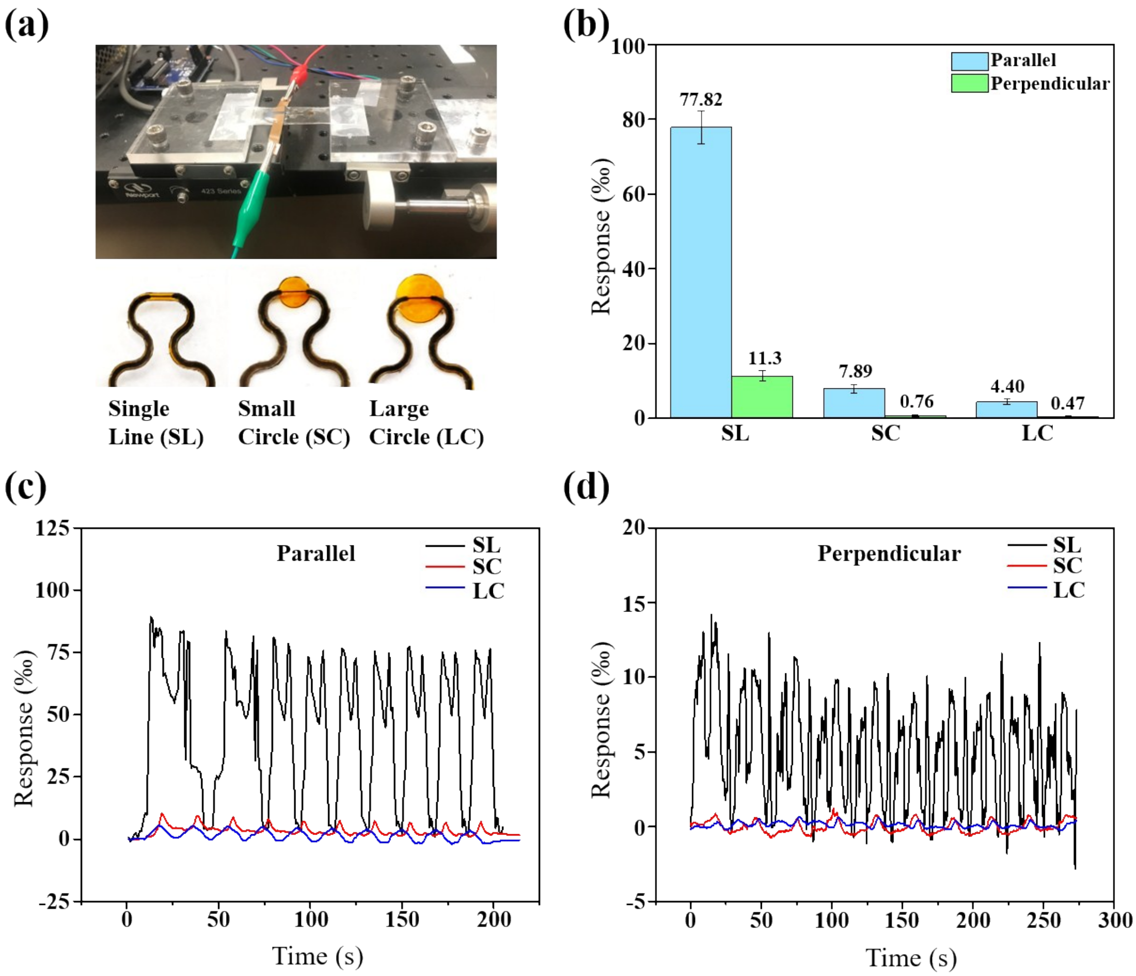

Figure S14. The stretchable LIG gas sensors with different strain isolation designs and their performance in the presence of cycling tensile strains. **(a)** Optical images of (top) the setup for tensile test and (bottom) three different PI substrate patterns for the strain isolation. **(b)** The average variation in the electrical resistance of the LIG gas sensor with different PI substrate designs under a tensile strain of 20 % applied in the parallel and perpendicular directions with respect to the LIG sensing line. The resistance fluctuation of the LIG gas sensor as a function of time for a tensile strain of 20 % in the **(c)** parallel and **(d)** perpendicular directions.

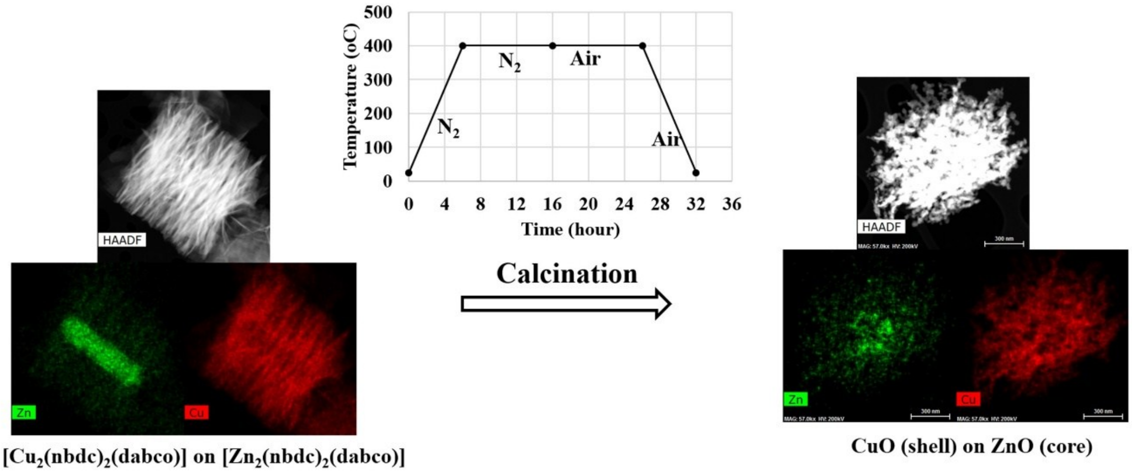

Figure S15. STEM image (HAADF) of $Cu_2(nbdc)_2(dabco)$-on-$Zn_2(nbdc)_2(dabco)$ metal-organic framework (MOF) with accompanying EDS spectrum images to show the elemental distribution. After calcination, the MOFs formed CuO-on-ZnO nanoparticles, where CuO shell was visible on ZnO core from the EDS spectrum images.

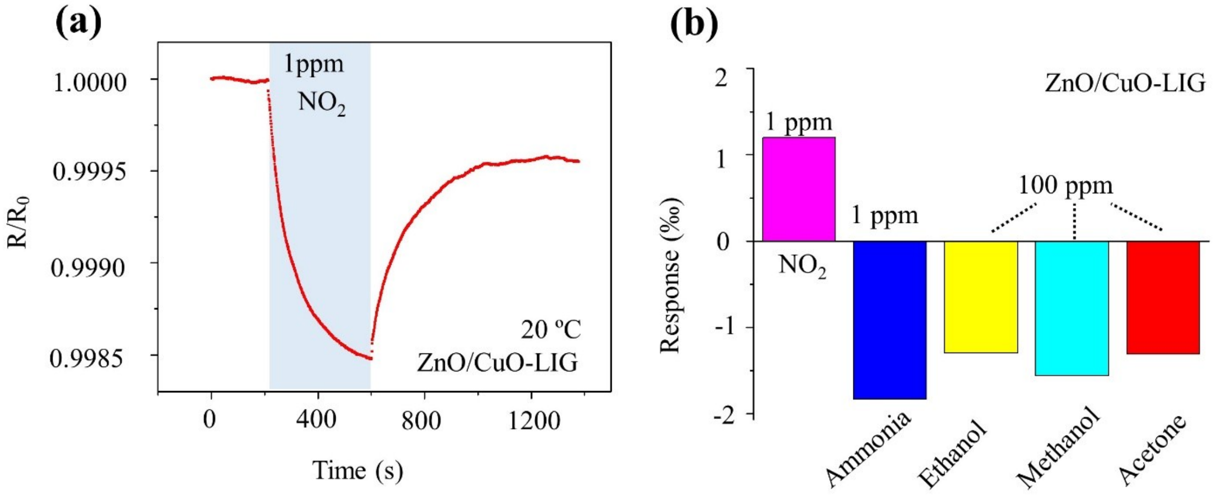

Figure S16. **(a)** Response and **(b)** selectivity of the ZnO/CuO-LIG gas sensor, in which ZnO/CuO core/shell nanomaterials were dispersed on LIG.